8-2021

Nitrogen-Doped Carbon Fiber Ultramicroelectrodes as Electrochemical Sensors for Detection of Hydrogen Peroxide

Eric Wornyo
East Tennessee State University

Nitrogen-Doped Carbon Fiber Ultramicroelectrodes as Electrochemical Sensors for Detection of Hydrogen Peroxide

---

A thesis

presented to

the faculty of the Department of Chemistry
East Tennessee State University

In partial fulfillment

of the requirements for the degree

Master of Science in Chemistry

---

by

Eric Sedom Wornyo
August 2021

Dr. Gregory W. Bishop, Chair
Dr. Dane W. Scott
Dr. Marina Roginskaya

Keywords: Ultramicroelectrode, nitrogen doping, carbon fiber, electrochemical sensing

ABSTRACT

Nitrogen-Doped Carbon Fiber Ultramicroelectrodes as Electrochemical Sensors for Detection of Hydrogen Peroxide

by

Eric Sedom Wornyo

Carbon fiber ultramicroelectrodes (CF-UMEs) are commonly used as electrochemical probes and sensors due to their small size, fast response, and high signal-to-noise ratio. Surface modification strategies are often employed on CF-UMEs to improve their selectivity and sensitivity for desired applications. However, many modification methods are cumbersome and require expensive equipment. In this study, a simple approach known as soft nitriding is used to prepare nitrogen-doped CF-UMEs (N-CF-UMEs). Nitrogen groups introduced via soft nitriding act as electrocatalytic sites for the breakage of O-O bonds during the reduction of peroxides like H_2O_2, a common target of biosensing strategies. Voltammetric studies confirm that, compared to CF-UMEs, N-CF-UMEs possess enhanced electrocatalytic activity towards H_2O_2 reduction as evidenced by an increase in current and positive shift in onset potential for the reaction. N-CF-UMEs also proved capable for amperometric detection of H_2O_2, exhibiting good linear response from 0.1 to 5.6 mM at -0.4 V vs. Ag/AgCl.

DEDICATION

This research work is dedicated to my late dad, Mr. Daniel Doh and my ever-supportive mom, Mrs. Florence Doh.

ACKNOWLEDGMENTS

My first and foremost thanks go to God Almighty for His guidance and protection throughout my studies.

I sincerely thank and appreciate my research advisor, Dr. Gregory W. Bishop for his patience, guidance, training, and knowledge throughout this research and my study period at ETSU. To my committee members, Dr. Dane W. Scott, and Dr. Marina Roginskaya, thank you so much for your invaluable contributions, advice, suggestions, and corrections throughout my research. I also thank my lab mates Ivy Antwi, Emmanuel Nkyaagie, and Emmanuel Preprah for their contributions and efforts throughout my research.

Finally, I would like to acknowledge the American Chemical Society Petroleum Research Fund (Award #58123 – UN15) for providing financial support for this research work, the East Tennessee State University RDC Grant Number 21-012M for funding this research, and the ETSU Chemistry Department for the Margaret Sells endowment scholarship award.

TABLE OF CONTENTS

ABSTRACT 2

DEDICATION 3

ACKNOWLEDGMENTS 4

LIST OF FIGURES 7

LIST OF ABBREVIATIONS 8

1. CHAPTER 1. INTRODUCTION 9

Ultramicroelectrodes 9

Applications of Ultramicroelectrodes 11

Fabrication and Modification of Ultramicroelectrodes 13

Hydrogen Peroxide Sensing Using Ultramicroelectrodes 15

Hydrogen Peroxide Sensing Using Carbon Fiber UMEs (CF-UMEs) and Modified CF-UMEs 16

Nitrogen Doping 19

Research Objectives 22

2. CHAPTER 2. EXPERIMENTAL 23

Materials 23

Nitriding Carbon Fiber 23

Fabrication of Carbon Fiber Ultramicroelectrodes 24

Characterization of UMEs 25

Hydrogen Peroxide (H_2O_2) Reduction 26

Amperometric Detection of Hydrogen Peroxide (H_2O_2) 27

3. CHAPTER 3. RESULTS AND DISCUSSION 28

Characterization of UMEs 28

Response of CF-UMEs and N-CF-UMEs in Aerated and De-aerated PBS Solutions 29

Comparison Between Solution-Based and Solid Urea Nitriding Methods 30

CF-UMEs and N-CF-UMEs Response towards Hydrogen Peroxide Reduction 33
Amperometric Detection of H_2O_2 Using CF-UMEs and N-CF-UMEs 35
4. CHAPTER 4. CONCLUSION AND FUTURE WORK 38
Conclusion 38
Future Work 39
5. REFERENCES 40
VITA 48

LIST OF FIGURES

Figure 1. Fabrication of Carbon fiber ultramicroelectrodes 25

Figure 2. Representative cyclic voltammograms showing the electrochemical response of electrodes in 0.5 mM FcMeOH containing 0.1 M KCl used for estimating electrode size. 28

Figure 3. Representative cyclic voltammograms in aerated and de-aerated PBS pH 7.4 solution vs Ag/AgCl. 30

Figure 4. Representative cyclic voltammogram in PBS pH 7.4 solution vs Ag/AgCl. 31

Figure 5. Representative cyclic voltammograms of varying concentrations of H_2O_2 in PBS pH 7.4 vs Ag/AgCl. 34

Figure 6. Effect of UME size on CV current density associated with reduction of H_2O_2 at -0.4 V. 35

Figure 7. Amperometry detection of H_2O_2 in PBS pH 7.4 at -0.4 V vs. Ag/AgCl. 36

Figure 8. Representative calibration curve for amperometric detection of H_2O_2 in PBS pH 7.4 at -0.4V vs. Ag/AgCl. for N-CF-UME (5.1 µm) 37

LIST OF ABBREVIATIONS

BDD	Boron-doped diamond
CF-UME	Bare carbon fiber ultramicroelectrode
CNT	Carbon nanotube
CV	Cyclic voltammetry
CVD	Chemical vapor deposition
DNA	Deoxyribonucleic acid
DFT	Density functional theory
EC-SPR	Electrochemical surface plasmon resonance
FcMeOH	Ferrocene methanol
GCE	Glassy carbon electrode
GrNR	Graphene nanoribbon
Hb	Hemoglobin
HRP	Horseradish peroxide
ID	Internal diameter
KCl	Potassium chloride
$NaBH_4$	Sodium borohydride
NADPH	Nicotinamide adenine dinucleotide phosphate
N-CF-UME	Nitrogen-doped carbon fiber ultramicroelectrode
N-CNT	Nitrogen-doped carbon nanotube
N-GrNR	Nitrogen-doped graphene nanoribbon
N-SPCE	Nitrogen-doped screen-printed carbon electrode
NPs	Nanoparticles
OD	Outside diameter
ORR	Oxygen reduction reaction
PB	Prussian blue
PBS	Phosphate buffer saline
RP	Ruthenium purple
SECM	Scanning electrochemical microscopy
SEE	Single entity electrochemistry
S/N	Signal to noise ratio
SPCE	Screen printed carbon electrodes
SWCNT	Single-walled carbon nanotube
UME	Ultramicroelectrode
UMEAs	Ultramicroelectrode arrays
VA-NCNTs	Vertically aligned nitrogen doped carbon nanotubes
XPS	X-ray Photoelectron Spectroscopy

CHAPTER 1. INTRODUCTION

Ultramicroelectrodes

Ultramicroelectrodes (UMEs) are generally defined as electrodes that have a critical dimension (e.g., the radius of a disk-shaped electrode, width of ring or band electrode, etc.)[1] to be ≤25 μm in size.[2,3] These small electrodes have faster double-layer charging and high mass transport rates than typical macroelectrodes[4], which have dimensions on the order of tens of micrometers to centimeters.[5] UMEs produce steady-state responses, exhibit fast response times, and small currents that fall within the pico- to nano-amperes range.[5] The small currents supported by UMEs provide a key advantage because small currents translate lower ohmic effects (e.g., ohmic or iR potential drop), and thus enable electrochemical measurements to be carried out in non-polar solvents (e.g., organic solvents with low supporting electrolyte concentrations).[5,6] The small currents at these electrodes also makes them essentially non-destructive to the species that are undergoing electrolysis.[6,7]

The small sizes of UMEs allow very effective mass transport of species to the electrode surface, which enables steady-state responses of diffusible redox-active species to be observed in typical voltammetric experiments.[5,8] Sigmoidal-shaped responses observed in cyclic voltammetry experiments of UMEs are indeed like those of rotating disk macroelectrodes that require rotation of several thousands of revolutions per minute to exhibit steady-state behavior.[5,9] The rapid response to changes in the applied potential and fast achievement of steady-state allows the monitoring of electrochemical processes on a microsecond or a nanosecond timescale. In comparison, conventional macroelectrodes can typically only measure electrochemical processes on a millisecond timescale. This feature of UMEs makes them useful in the studies of

very rapid homogenous and heterogeneous electron transfer processes, and redox reactions that involve short-lived intermediates.[5,10]

In the early 1980s, Wightman et al. demonstrated the unique properties of UMEs compared to conventional macro electrodes.[7] He fabricated UMEs < 10 μm in radius to make chemical measurements of neurotransmitters (e.g., dopamine, serotonin, epinephrine, and norepinephrine) in the brains of mammals. While these chemicals are easily oxidized on the surface of carbon electrodes, their confinement and fast transport across synapses make them impossible to measure with conventional macroelectrodes.[7]

Independent work by Fleischmann[2] around the same time as Wightman's studies indicated that UMEs exhibit very small currents (i.e., approximately 10^{-17} A which corresponds to 10 e^-/s). Also, there is a reduction of capacitive charging currents to very negligible proportions at UMEs. The capacitive charging current is a restriction factor in all transitory quantitative electrochemical measurements as it is considered background current (or noise) related to non-Faradaic processes involved in establishing the electrical double-layer rather than the signal current associated with electron transfer between the electrode and redox-active analyte species of interest. Fleischmann indicated that the small sizes of UMEs enable an increase in the mass transport rate of species to and from the electrode surface. Due to the reduced capacitive charging currents and the increase in mass transport rates, UMEs show an outstanding signal-to-noise ratio (S/N).[2] This feature of UMEs allows electrochemical measurements of a substrate of low concentrations to be made, resulting in lower detection limits than those obtained with traditional macroelectrodes. Due to the above outstanding features and benefits of UMEs, they continue to be widely used and are employed in a range of applications related to sensing and imaging.

Applications of Ultramicroelectrodes

While UMEs have continued to be employed for *in vivo* measurements of neurotransmitters in the brains of mammals since their original development by Wightman and Fleischmann,[2,7] their unique features and benefits make them well-suited for many other applications. For example, Bard et al. employed UMEs as probes in scanning electrochemical microscopy (SECM) applications beginning in the late 1980s.[11] In their work, a UME tip (diameter 10 µm) having electrolysis current flowing through it was immersed in a solution and moved above the surface of a substrate using a computer-controlled positioning system. The UME tip was positioned on an x, y, and z tripod piezoelectric scanner with the substrate held at an angle of 45° to the UME tip. The substrate was supported by an x-y movable stage and moved by two piezoelectric translators that were controlled by a computer. This helped to characterize the structural features of the substrate as well as detecting products that are electrogenerated at the substrate at an applied constant potential. They observed that making electrodes with small sizes presents a major benefit in enhancing resolution. In more recent work by Bard et al.,[12] they mentioned the importance of fabricating UMEs tips with sizes in micrometer and sub-micrometer range. This allows the measurements of fast homogeneous and heterogeneous rate constants as well as for high spatial resolutions. They, therefore, fabricated carbon paste UMEs of diameters between 285 nm and 10 µm having a very small insulating sheath for SECM measurements. These probes produced satisfactory SECM curves and allowed an approaching distance of up to 200 nm towards the substrate of interest. Similarly, Foord et al. fabricated boron-doped diamond (BDD) UME tips of 1 µm to 25 µm for SECM applications.[13] In their work, the approach curves and SECM images of the electrochemical activities of immobilized *E.*

coli were obtained using the tips of BDD UMEs. The results obtained showed satisfactory performance of BDD UMEs for imaging applications in biological media.

UMEs have also facilitated the study of single nanoparticles and other single entities. The impact of single nanoparticles on the surface of UMEs can be observed through measurements of current or potential.[14] The small sizes of UMEs decrease particle collision frequencies and reduce the baseline noise significantly such that single collision events can be observed by monitoring current or potential as a function of time. For example, Bard et al. demonstrated that the distribution of particle size and estimation of nanoparticles concentrations and diffusion coefficients could be determined from current versus time signals generated by collisions of single nanoparticles with UMEs.[15] In their work, 10 µm carbon, gold, and platinum UMEs, as well as 25 µm gold and platinum UMEs, were used and single nanoparticle collisions were observed via cyclic voltammetry and chronoamperometry after the injection of platinum (Pt) colloids into an electrode bath solution. Collisions and adhesion of single Pt nanoparticles with the UME coincided with transient increases in current. These signals were the result of electrochemical reduction of protons or the oxidation of hydrazine which were only possible when the electrocatalytic nanoparticle was in contact with the relatively inert UME. In another study by Bard et al., the collision of single iridium oxide (IrO_2) nanoparticle having an approximate diameter of 2 nm was observed at the surface of a $NaBH_4$ treated Pt UME.[16] An increase in current was observed due to the electrocatalytic oxidation of water when IrO_2 nanoparticle makes contact with the UME and briefly sticks to it. Single metal nanoparticle collisions were also successfully observed using gold (Au) UME (5 µm diameter) by potentiometric measurement.[17] Changes in open circuit potential of Au UME in hydrazine solution resulted when Pt nanoparticles (4 nm) collides with the Au UME, which were related to

the size of NPs, Au UME, the redox process, and the concentration of hydrazine. Since the pioneering studies of single nanoparticles by Bard and others[15,16,17], UMEs have found increasing use in the new and rapidly developing field of single entity electrochemistry (SEE).

Fabrication and Modification of Ultramicroelectrodes

For UMEs to achieve the low detection limits, high sensitivities and selectivities for desired electrochemical applications, various fabrication, and modification strategies have been employed. UMEs can be fabricated from conductive materials using several different techniques, which can result in different electrode geometries, including disk shape[18,19] , ring-disk[20,21] , hemispherical[22,23], finite conical[24] and inlaid ring[25,26]. One common method for fabricating UMEs involves inserting and sealing a conductive material (e.g., metal wire, carbon fiber, etc.) in an insulating material[27] (e.g., glass capillary tube, polymer, etc.). One popular technique for pulling and sealing the conductive material is through the use of a laser-based micropipette puller.[28]

UMEs prepared with a micropipette puller possess tapered ends containing the conductive material sealed in the glass sheath. Further sealing of the tip can be done using a torch, heated filament, or laser. Electrical contact with the conductive filament is made by inserting a metal wire in the open side of the glass capillary.[29] Exposure of the conductive material is achieved via mechanical polishing of the tip on a grit paper, chemical etching, or other means.[19] Conductive materials commonly used for fabrication of UMEs include metal wires (e.g., Au, Pt, and Ag) of a few to tens of micrometers in diameter as well as carbon materials.[30] For example, Wightman used the micropipette pulling method to prepare 6-12 μm carbon UMEs. After the fiber was positioned and exposed in the glass capillary, epoxy was used to create a strong seal at the tip.[7] McCreery et al. employed a similar strategy but used wax to

seal the fiber in the capillary, resulting in 12 μm in diameter cylindrical electrodes.[31] In another similar fabrication technique, Danis et al. used carbon fiber and other conductive materials that include platinum, gold, mercury, and silver to prepare UMEs.[19]

After successful fabrication, UMEs can be used for direct measurements of electroactive species. However, surface modification of UMEs is a common strategy to enhance sensitivity and selectivity, and thus optimize UME properties for a particular application. For example, Nenad et al. immobilized nucleic acids on the surface of UMEs[32] for the detection of single-base mutations in DNA. In other UMEs modifications, Carrera et al. modified carbon fiber UMEs with Au nanoparticles for arsenic determination in water.[33] The modified electrode provided a high selectivity towards arsenic with a detection limit of 0.9 μg/L and sensitivity of 0.0176 nA μg/L. Orozco et al. also modified Au ultramicroelectrode arrays (UMEAs) using Au nanoparticles with horseradish peroxidase enzyme (HRP) immobilized onto it.[34] The resulting biosensor was used for the detection of catechol which resulted in a linear response of 0.1 mM to 0.4 mM and a detection limit of 0.05 mM. Li et al. modified a Pt disk UME with Prussian blue (PB) film to investigate the electrocatalytic reduction of H_2O_2 from glucose oxidase (GOx) enzyme.[35] SECM images obtained using the modified electrode showed a concentration profile of the reacting products around the enzyme. Qing et al. modified an ensemble of carbon fiber UMEs with carbon nanotubes for the study of the electrochemical properties of dopamine (DA).[36] The detection limit was 2.0 nM, and the linear range extended from100 nM to 0.08 mM. Surface modifications of UMEs continue to be of great importance as new strategies in this regard can enhance electrode response, limit interferences, and/or enable new applications such as the sensing of hydrogen peroxide (H_2O_2).

Hydrogen Peroxide Sensing Using Ultramicroelectrodes

While UMEs continue to find extensive use in electrochemical measurements, SECM applications, and for *in vivo* detection of important neurotransmitters like dopamine, they have also been recently employed to measure other important electroactive species like hydrogen peroxide (H_2O_2), which is a product of many oxidase enzyme reactions and a common target of biosensing strategies. The detection of aging mechanism, cellular signaling, and various oxidase enzymes (e.g., glucose oxidase, cholesterol oxidase, nicotinamide adenine dinucleotide phosphate (NADPH) oxidase, oxalate oxidase, lactate oxidase, glutamate oxidase, lysine oxidase, urate oxidase) can indirectly be done using H_2O_2 as an analyte.[37,38] H_2O_2 is also recognized especially in the brain as a useful intercellular and intracellular messenger.[39] Therefore, the research on H_2O_2 sensing and detection is of significance in both industry and academics.

Various methods have been employed for the detection and sensing of hydrogen peroxide. These methods include electrochemical surface plasmon resonance (EC-SPR) spectroscopy, ultraviolet spectroscopy, chemiluminescence, titrimetry, and electrochemistry.[40,41,42] Among these methods, electrochemical detection of hydrogen peroxide has gained much interest due to its sensitivity, selectivity, simplicity, accuracy, and low cost.[43,44] Electrochemical detection of H_2O_2 is usually done by applying a potential at which either the oxidation (equation 1) or reduction of H_2O_2 (equation 2) occurs. The resulting current associated with the reaction is measured via amperometry or voltammetry.[45,46] The standard electrode potential (E°) for these half-reactions are +0.682 V and +1.776 V, respectively.[47]

$$O_2(\mathrm{g}) + 2H^+ + 2e^- \rightleftharpoons H_2O_2 \quad (1)$$

$$H_2O_2 + 2H^+ + 2e^- \rightleftharpoons 2H_2O \quad (2)$$

While the E° values suggest that the oxidation and reduction of H_2O_2 should be easy, in reality, these reactions have larger overpotentials and therefore a lot of times electrocatalysts are required. For example, for the H_2O_2 reduction, Zheng et al[48] found the reduction of H_2O_2 to H_2O at Au electrodes required an overpotential of about 1.4 V. They did not start to see the reduction of H_2O_2 until at a potential of +0.35 V vs. real hydrogen electrode (RHE).

Over the years, researchers have focused on developing novel electroactive materials to enhance the sensitive electrochemical detection of H_2O_2.[49,50] Miniaturization of electrodes allows for the measurements of H_2O_2 in very small sample volumes and at low concentrations.[51,52] Dantas et al. fabricated a 12.5 µm Copper (Cu) UME for the cathodic reduction of H_2O_2 in phosphate buffer solutions pH 7.0.[53] They reported amperometric responses of H_2O_2 at -0.2 V with a detection limit of 2.7 µM with a linear range of 0.015 mM to 1.82 mM. In a research work by Stuart et al, a 25 µm mesoporous Pt UME was also used for the detection of H_2O_2 in phosphate buffer solution pH 7.[54] A linear response was obtained for concentrations between 0.02 mM to 40 mM with a detection limit of 4.5 µM and sensitivity of 2.8 mA $mM^{-1}cm^{-2}$.

Fabrication of amperometric UMEs for H_2O_2 sensing is usually done using metal wire and carbon fiber of which noble metals like Pt provides better electrocatalytic activities towards the reduction and oxidation of H_2O_2.[55]However, the high cost of these noble metals limits their application in making H_2O_2 UMEs amperometric sensors.[54] In comparison, carbon fiber UMEs are an alternative for making H_2O_2 sensors due to their relatively low cost, chemical inertness, and biological compatibility.[56]

Hydrogen Peroxide Sensing Using Carbon Fiber UMEs (CF-UMEs) and Modified CF-UMEs

Sanford et al. used CF-UME for the voltammetric detection of H_2O_2 oxidation in the brain of a rat that has been sliced and kept in a Tris buffer solution.[57] The detection limit was

obtained as 1.9 ± (0.1) µM and a linear response between 0 mM to 2 mM. In relation to modification of UMEs, CF-UMEs are also modified to enhance the sensing and detection of H_2O_2. For example, Mustafa et al. electrochemically detected H_2O_2 by comparing measurements relating to an unmodified carbon fiber electrode (CFE) and a nanoporous CFE.[58] Surface modification was done by heat-treating the electrode using a micro forge under a microscope making it nano-porous. Cyclic voltammograms were obtained for both oxidation and reduction of varying concentrations of H_2O_2 in PBS solution for both electrodes. The results showed an oxidation current of H_2O_2 at the nanoporous CFE to be approximately 4 times higher compared to the unmodified CFE. Chronoamperometry results for H_2O_2 oxidation at the nanoporous CFE produced a detection limit of 0.57 µM. Also, CV for the reduction current of H_2O_2 at the nanoporous CFE showed approximately 2.22 times increase in the reduction current compared to the unmodified electrode. Barbosa et al. reported a modification of carbon fiber microelectrode (CFM) using ruthenium purple (RP) for the detection of H_2O_2 concentration dynamics in brain tissue extracellular space.[59] From the study, a linear response was observed within 2 µM to 500 µM H_2O_2 concentration with a sensitivity of 0.98± (0.37) µA μM^{-1} cm^{-2}.

Modification of CF-UMEs to enhance H_2O_2 detection is also achieved using metal nanoparticles.[60,61]. For example, Maidment et al. reported a modification of carbon fiber microelectrode (CFME) with Pt-nanoparticles for the selective detection of H_2O_2.[61] Using these electrodes, a sensitivity of 7711± (587) µA mM^{-1} cm^{-2}, a detection limit of 0.53±(0.16) µM (S/N=3) and a linear range between 0.8 µM to 8.6 mM were reported. Similarly, Minbo et al. deposited bimetallic Au Ag nanoparticles onto a carbon-fiber microelectrode (CFME) for H_2O_2 detection.[62] Results from the detection of H_2O_2 showed a sensitivity of 1,319 µA mM^{-1} cm^{-2} for a

0 μM to 55 μM linear range, and a sensitivity of 273 μA mM^{-1} cm^{-2} for a 55 μM to 2775 μM linear range with a detection limit of 0.12 μM for both measurements.

Modification of CF-UMEs with enzymes and other biomolecules is another strategy at enhancing the detection of H_2O_2. For example, Michael et al. modified the surface of a carbon fiber electrode with a cross-linked redox polymer (RP) film that contained horseradish peroxidase (HRP) enzyme for the detection of H_2O_2 in the brains of anesthetized rats to measure neurochemical activities via amperometry.[63] The detection limit was found to be 285± (60) nM (S/N=3). Wang et al. also modified carbon fiber microelectrode (CFME) for the reduction of H_2O_2 based on reduced hemoglobin (Hb) and single-walled carbon nanotubes (SWCNTs).[64] Results from the electrochemical measurement of H_2O_2 reduction produced linearity for concentrations from 0.51 μM to 10.6 μM with a detection limit of 0.23 μM.

Even though the above modification strategies have been largely successful in the sensing and detection of H_2O_2 resulting in high sensitivity and selectivity, most are cumbersome and require expensive materials, equipment, and expertise. The development of novel, low-cost, simple methods for modifying CF-UMEs that gives the electrode superior electrocatalytic activity for electrochemical sensing of H_2O_2 remains a research topic of much interest. One strategy that has shown promise for enhancing the electrocatalytic activity of carbon materials towards H_2O_2 reduction involves doping the carbon surface with heteroatoms like nitrogen.

Table 1. Comparison of Some Modified Carbon Fiber UMEs towards H_2O_2 Sensing

Electrode	Linear range (μM)	Sensitivity (μA $mM^{-1}cm^{-2}$)	Detection Limit (μM)	Applied potential (V)	Ref.
Nanoporous CFE	0 - 50	n/a	0.57	+0.8	58
Nanoporous CFE	50 -1000	n/a	n/a	-0.6	58
RP-CFM	2 - 500	980 ± (370)	0.07 ± (0.04)	-0.1	59
Pt-CFME	44 - 12300	n/a	44	-0.1	8
Pt-CFME	0.8 - 8600	7711 ± (587)	0.53 ± (0.16)	+0.7	61
Au Ag-CFME	0 - 55	1319	0.12	-0.8	62
Au Ag-CFME	55 - 2775	273	0.12	-0.8	62
HRP-CFE	0 - 10	n/a	0.285± (0.06)	-0.1	63
Hb-SWCNTs-CFE	0.51 - 10.6	n/a	0.23	-0.35	64

Nitrogen Doping

Heteroatom doping of carbon is the incorporation of atoms of other elements such as nitrogen on the surface of graphite or other carbon materials. N-doped carbon materials are made from methods such as nitrogen plasma treatment of carbon nanofibers[70], graphene[65],low-temperature hydrothermal treatment of graphene nanoribbons in ammonium hydroxide[66], low-temperature annealing of mesoporous carbon, carbon black, and activated carbons using urea (soft nitriding)[67], and the pyrolysis of iron (II) phthalocyanine (FePc).[68,69] The doping of carbon

materials with nitrogen atoms introduces free electrons that facilitate the breakage of O-O bonds at the electroactive sites[70,71] which is an important step during H_2O_2 reduction.

To understand the electrocatalytic activity of nitrogen-doped carbon materials towards the breakage of O-O bond, experimental observations, and quantum mechanics calculations of oxygen reduction reactions (ORR) using vertically aligned nitrogen-doped carbon nanotubes (VA-NCNTs) arrays were performed by Dai et al.[69,72] They observed that with the quantum mechanical calculations together with density functional theory (DFT), the carbon atoms adjacent to the nitrogen dopants possessed a positive charge density to neutralize the electron affinity of nitrogen atom. They suggested that the chemisorption mode of O_2 could change from its regular end-on adsorption at the surface of carbon nanotubes (CNT) to side-on adsorption at the nitrogen-doped carbon nanotubes (NCNT) due to the charge delocalization induced by nitrogen. This parallel adsorption of O_2 (where the bond is just above the nitrogen site) could weaken the O-O bond which, in turn, facilitates ORR at NCNT electrodes. Also, Wu et al[73] carried out a DFT study on the effects that nitrogen groups in graphene have on H_2O_2 reduction. By simulating the adsorption processes and calculating the reversible potential of the reduction of H_2O_2, they observed that H_2O_2 adsorption on N-graphene happened through physisorption resulting in the breakage of O-O bond and formation of the O-C bond and H_2O. They suggested that the reactivity of N-doped graphene followed the following order: pyridinic N > pyrrolic N > graphitic N according to the computations of their relative energy and the onset potential for the reduction of H_2O_2.

Recent work by Minbo et al.[66] showed that nitrogen-doped carbon nanotubes (N-CNTs) and nitrogen-doped graphene nanoribbons (N-GrNRs) produced an enhanced electrocatalytic activity towards H_2O_2 sensing compared to carbon nanotubes (CNTs) and graphene nanoribbons

(GrNRs). The enhanced electrocatalytic activity of N-CNTs and N-GrNRs compared to CNTs and GrNRs was attributed to the nitrogen groups that facilitated the breaking of the O-O bond[74] in H_2O_2. N-GrNRs showed a linear response to H_2O_2 within a 5 μM to 2785 μM concentration range and a detection limit of 1.72 μM at a potential of -0.4 V against an Ag/AgCl reference electrode. Lin et al. also reported nitrogen doping of graphene (N-doped graphene) by nitrogen plasma treatment to introduce nitrogen groups (pyridinic N, pyrrolic N, and quaternary N) on graphene.[74] They indicated that the percentage of nitrogen on graphene ranged from 0.11% to 1.35% by controlling the exposure time. Results from electrochemical reduction of H_2O_2 response at N-doped graphene showed a positive potential shift of about 0.4 V with approximately 20 times current increase compared to the response from a glassy carbon electrode (GCE). Stevenson et al. also demonstrated the benefits of nitrogen doping by comparing the electrochemical behavior of nitrogen-doped carbon nanotubes (N-CNTs) and carbon nanotubes (CNTs) towards the oxidation and reduction of H_2O_2.[45] The anodic sensitivity of N-CNTs was 830 mA M^{-1} cm^{-2} and a detection limit of 0.5 μM at 0.05 V. The cathodic sensitivity was 270 mA M^{-1} cm^{-2} and a detection limit of 10 μM at -0.25 V using a Hg/Hg_2SO_4 reference electrode.

In previous research by our group, Amoah[75] demonstrated the benefit of nitrogen doping of chemical vapor deposited carbon (CVD) UMEs towards H_2O_2 reduction. In his work, nitrogen-doped CVD UMEs showed a high electrocatalytic activity by a significant increase in the reduction current compared to unmodified CVD UMEs. There was a shift to a more positive onset potential at the nitrogen-doped CVD UMEs compared to unmodified CVD UMEs.
In a separate work by Ogbu et al,[76] nitrogen-doped screen-printed carbon electrodes (N-SPCEs) were prepared from graphite that was modified using Liu et al[67] method which is a simple soft

nitriding based on thermal decomposition of urea in the presence of carbon materials. N-SPCEs showed an enhanced electrocatalytic activity towards the reduction of H_2O_2 at -0.4 V compared to bare SPCEs. Using these electrodes, the method had a sensitivity of 264 μA $mM^{-1}cm^{-2}$, a detection limit of 2.5 μM, and a linear range between 0.020 mM to 5.3 mM. Affadu-Danful[77], a previous member of this group, showed that the same kind of soft nitriding technique could be used to modify carbon fiber and make nitrogen-doped carbon fiber ultramicroelectrodes (N-CF-UMEs). In his work, XPS showed that the nitrogen groups were present on the nitrided fiber. However, the electrodes were used for the deposition of metal nanoparticles and not for H_2O_2 sensing.

Research Objectives

Nitrogen-doped carbon materials have emerged as promising materials for H_2O_2 detection. These heteroatoms change the electron density in carbon materials leading to an improvement in the breakage of the O-O bond which is a critical step in H_2O_2 reduction. [71,66,74] Previous work in this group has shown that recently reported simple nitriding strategy[67] for modifying carbon materials can be used to make screen printed electrodes and N-CF-UMEs. Nitrogen-doped screen-printed electrodes from carbon have been investigated and have properties that are in line with these benefits reported.[76] Previous students have researched with carbon fiber and shown that the soft nitriding process works on carbon fiber as well by introducing nitrogen groups.[77]

The goals are to use these N-CF-UMEs to investigate their abilities as sensors for H_2O_2. Therefore, I will be comparing unmodified or bare carbon fiber UMEs (CF-UMEs) and N-CF-UMEs towards H_2O_2 reduction reaction with the possibilities of making H_2O_2 amperometric sensors that could produce a high sensitivity with a low detection limit.

CHAPTER 2. EXPERIMENTAL

Materials

Ferrocene methanol (≥97%), potassium chloride (99+%), and Urea (99+%) were purchased from Sigma-Aldrich. Ethanol (ethyl alcohol) was purchased from Greenfield global USA Inc. Acetone and hydrogen peroxide (30% w/v) were obtained from Fisher Scientific. Phosphate buffer saline (PBS) tablet was obtained from MP biomedicals, LLC. Ultra-high purity nitrogen gas was obtained from Airgas. Silver conductive adhesive paste was purchased from Beantown Chemicals (Hudson, NH). Ag/AgCl reference electrode was obtained from CH instruments, Inc. Borosilicate glass capillary tubes (O.D: 1.0 mm, I.D: 0.50 mm, and length: 10 cm) were purchased from Sutter instruments company (Novato, CA). Carbon fiber (7 µm in diameter) was purchased from Goodfellow Cambridge limited (Huntington, England). All solutions were prepared using 18.2 MΩ cm ultrapure water. The ultrapure water was made by passing deionized water through a Millipore synergy purifier.

Nitriding Carbon Fiber

Nitrogen doping of carbon fiber was carried out using a method employed by Liu et al[67] with some modification as previously documented.[77] In previous studies, X-ray photoelectron spectroscopy (XPS) results showed that this nitrogen doping procedure increased the nitrogen content on nitrided carbon fiber to approximately 3.5x higher than that of the bare carbon fiber.[77] The presence of nitride, amine or amide, ammonium, and pyridinic nitrogen groups were observed with the pyridinic nitrogen groups showing a significant increase compared to bare carbon fiber. Briefly, 1 g of commercially available carbon fiber (7 µm in diameter) was mixed with 1.5 g urea and heated in an oven to a temperature of 150 °C for 2 hours and further heated to 250 °C for another 4 hours. The annealed fiber was washed with ethanol and with ultra-pure

water. It was later dried in an oven at 60 °C overnight. In a similar nitriding process, a slight modification was attempted, thus carbon fiber was mixed with urea solution (0.4 M or 1.6 M) and heated to dryness using the same mass ratio of carbon fiber-to-urea and heating protocol.

Fabrication of Carbon Fiber Ultramicroelectrodes

Both bare and nitrogen-doped carbon fiber ultramicroelectrodes were fabricated by aspirating a single carbon fiber (7 µm in diameter) into a borosilicate glass capillary tube using a vacuum pump. The presence of the fiber in the capillary tube was verified using a Nikon microscope connected to a Pixelink CMOS camera and computer. The capillary tube containing the carbon fiber was clamped and pulled into two micropipettes using a laser-assisted micropipette puller instrument (Sutter P-2000). This resulted in the sealing of the fiber in the glass sheath. The following pulling program parameters (Heat:380, Filament: 3, Velocity:225, Delay: 0, Pull:0)[78] were applied until the two sides of the capillary separated. All the pulling parameters used on the micropipette puller are dimensionless and do not represent real temperature or velocity.

After pulling, a stainless-steel wire covered with silver conductive paste was inserted into the open end of the capillary tube to make electrical contact with the carbon fiber. Epoxy was applied to the open end of the capillary to ensure the wire does not lose connection with the carbon fiber. To expose the carbon fiber sealed in the capillary tube, the tapered end of the capillary tube was polished carefully using an abrasive paper due to the fragile nature of the electrode. To monitor the polishing progress, cyclic voltammetry (CV) measurements were carried out periodically. A two-electrode system was used for CVs with the UME serving as the working electrode and an Ag/AgCl electrode serving as both counter and reference electrode.[77] CV responses of the UME in a solution containing redox probe FcMeOH were obtained using a

Bioanalytical Systems (BAS) Epsilon electrochemical workstation in between polishing steps until a sigmoidal signal resulted, which is consistent with electrodes of <25 μm in size. In addition to CVs for evaluation of the polishing process, all electrochemical measurements were obtained with the BAS Epsilon and for all plots of electrochemical data, the US convention (e.g., positive currents correspond to cathodic processes and negative currents to anodic) was used.[79]

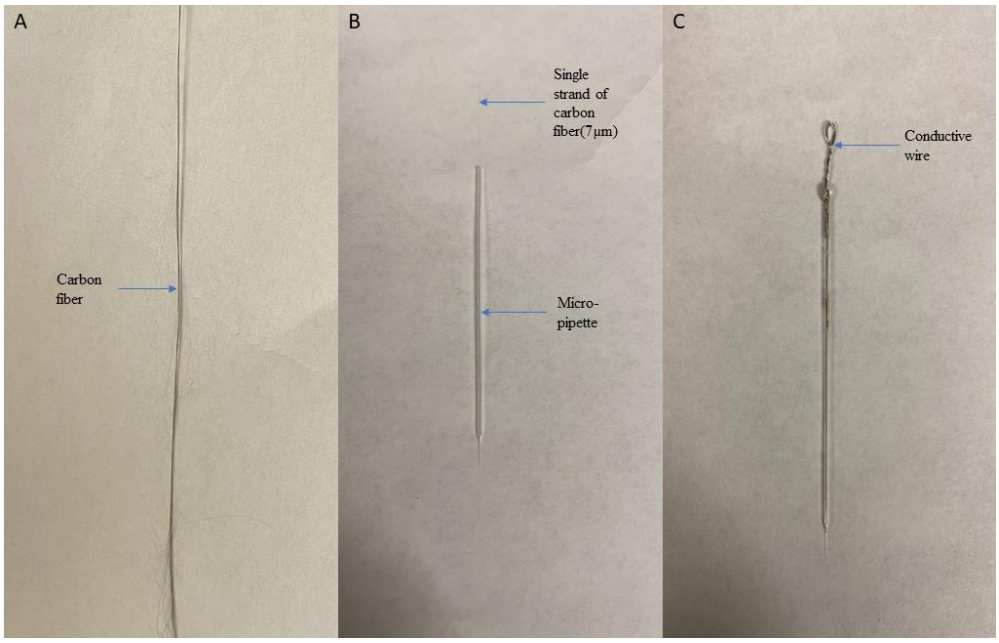

Figure 1. Fabrication of Carbon fiber ultramicroelectrodes (a) carbon fiber (b) a strand of carbon fiber aspirated into a borosilicate glass tube and pulled into a micropipette (c) conductive wire attached to carbon fiber using silver paste and sealed with epoxy at the open end to make CF-UMEs

Characterization of UMEs

Both bare carbon fiber and nitrogen-doped carbon fiber UMEs were characterized using cyclic voltammetry.[80] The redox probe used was 0.5 mM FcMeOH containing 0.1 M KCl as a supporting electrolyte. A potential of 0 mV to 450 mV and back to 0 mV was applied to the working electrode at a scan rate of 25 mV/s. The steady-state current (Iss) which is produced is directly related to the radius of the UME. The electrode radius is estimated using equation 3.[80,81]

$$I_{ss} = 4nFDRC \quad (3)$$

where n represents the number of electrons transferred in the redox reaction per mole of the reactant (1), F is the Faraday's constant (96485 C/mol), D is the diffusion coefficient (7.8×10^{-6} cm^2 /s) for FcMeOH, R is the radius of the electrode (cm) and C is the bulk concentration (mol/cm^3) of the redox molecule.[77]

Hydrogen Peroxide (H_2O_2) Reduction

Cyclic voltammetry (CV) was performed in a Faraday cage using a two-electrode[77] configuration with the carbon fiber electrodes serving as working electrodes and Ag/AgCl electrode serving a counter and reference electrode. To determine the electrocatalytic activity for the reduction of H_2O_2 for CF-UMEs and N-CF-UMEs, the potential of these working electrodes was scanned from 100 mV to -600 mV and back to 100 mV in a PBS solution pH 7.4 at a scan rate of 50 mV/s.[76] The background voltammograms were measured in both aerated and de-aerated PBS pH 7.4 solutions. The PBS solution was de-aerated by purging with nitrogen gas (N_2) for 20 minutes. CV measurements were taken for 5 mM, 10 mM, 15 mM, and 20 mM of H_2O_2 by spiking a 0.5 M H_2O_2 stock solution into the de-aerated PBS solution. The solution was held under an N_2 atmosphere during CV scans. CV behavior of UMEs in 0.5 mM FcMeOH containing 0.1 M KCl was determined and compared to the initial CV with the same redox probe to evaluate the possible effects of H_2O_2 experiments on electrode stability.

Electrodes that showed more than 5% variation in FcMeOH steady-state current were deemed too unstable for subsequent studies. The instability could be ascribed to incomplete sealing of electrodes or potential damage sustained between CV measurements. Only electrodes with less than 5% variation in FcMeOH steady-state current before and after H_2O_2 experiments were used in subsequent studies.

Amperometric Detection of Hydrogen Peroxide (H_2O_2)

Amperometry measurements were carried out using a three-electrode configuration in a Faraday cage with the carbon fiber electrodes serving as the working electrode, a platinum wire served as a counter electrode, and Ag/AgCl serving as the reference electrode.[76] Electrochemical measurements were carried out for injections of 0.1 mM, 0.4 mM, 0.9 mM, 1.6 mM, 2.6 mM, and 5.6 mM H_2O_2 in PBS pH 7.4. The PBS solution was purged with nitrogen for 20 minutes before the measurements and held under an N_2 atmosphere throughout the experiments. The measurement was carried at a reduction potential of -0.4 V[76] which is a common potential used for H_2O_2 reduction experiments and to prevent the possible interference with other reduction reactions by choosing a more negative potential.

CHAPTER 3. RESULTS AND DISCUSSION

Characterization of UMEs

CVs of both CF-UMEs and N-CF-UMEs in 0.5 mM FcMeOH containing 0.1 M KCl exhibited the expected sigmoidal responses.[80] For all electrodes used in these studies, sizes ranging from 3 µm to 7 µm calculated from steady-state current using equation 3 were used. [80,81]

For this study and all comparisons, only CF-UMEs and N-CF-UMEs that showed a sigmoidal shape (Figure 2) were used. Also, for all direct comparisons between electrochemical responses of CF-UMEs and N-CF-UMEs, only electrodes of similar sizes having a percent difference of no more than ±5% were used to avoid possible complications that may be attributed to size-related effects.

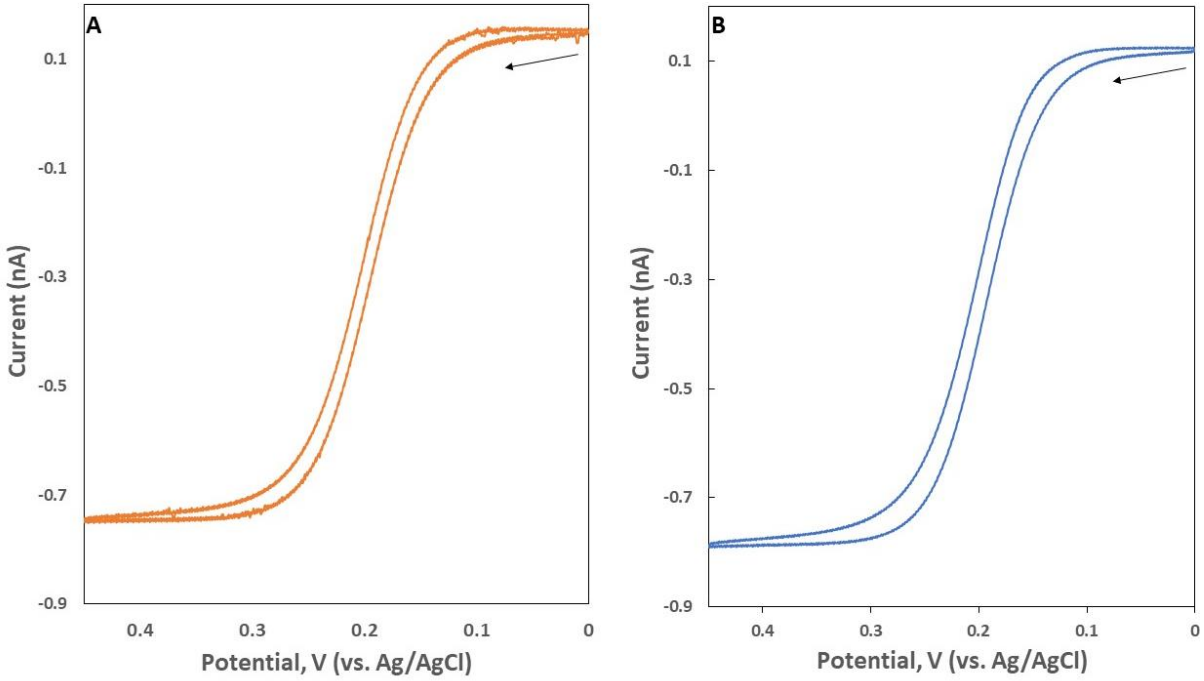

Figure 2. Representative cyclic voltammograms showing the electrochemical response of electrodes in 0.5 mM FcMeOH containing 0.1 M KCl used for estimating electrode size. (a) CF-UME (5.9 µm) (b) N-CF-UME (6.0 µm). The arrows show the direction of the forward scan.

Response of CF-UMEs and N-CF-UMEs in Aerated and De-aerated PBS Solutions

Like the ORR, the critical step in the reduction of H_2O_2 is the breakage of the O-O bond. [66,75] Therefore the presence of oxygen could interfere with the electrochemical detection of H_2O_2. To evaluate the behavior of CF-UMEs and N-CF-UMEs towards dissolved oxygen gas from air, CVs were obtained for both electrodes in aerated and de-aerated PBS (pH 7.4) (Figure 3). While both electrodes showed an increase in the current beginning at about -200 mV in the aerated solution due to the reduction of oxygen (O_2), N-CF-UME showed a significantly higher current of about 2.5 times compared to CF-UME. For both electrodes, no significant current was observed in the range of +0.1 V to -0.6 V vs. Ag/AgCl after the solution has been bubbled with nitrogen (N_2) for 20 minutes to remove dissolved air. The increase in current at both electrodes in the aerated solutions shows it is necessary to carry out the reduction of H_2O_2 in de-aerated PBS solutions to avoid possible interference due to the reduction of oxygen.

Based on CV results, both electrodes are capable of reducing oxygen in aerated PBS solutions but N-CF-UMEs enhances the reduction of H_2O_2 significantly compared to CF-UMEs. It is therefore possible for these N-CF-UMEs to be used in electrochemical reactions where ORR is desired. Further experiments could be done on dissolved oxygen to establish the electrocatalytic properties of N-CF-UMEs towards ORR. The most common kind of applications will be in fuel cells and for that, a high surface area electrode will be needed. [71]

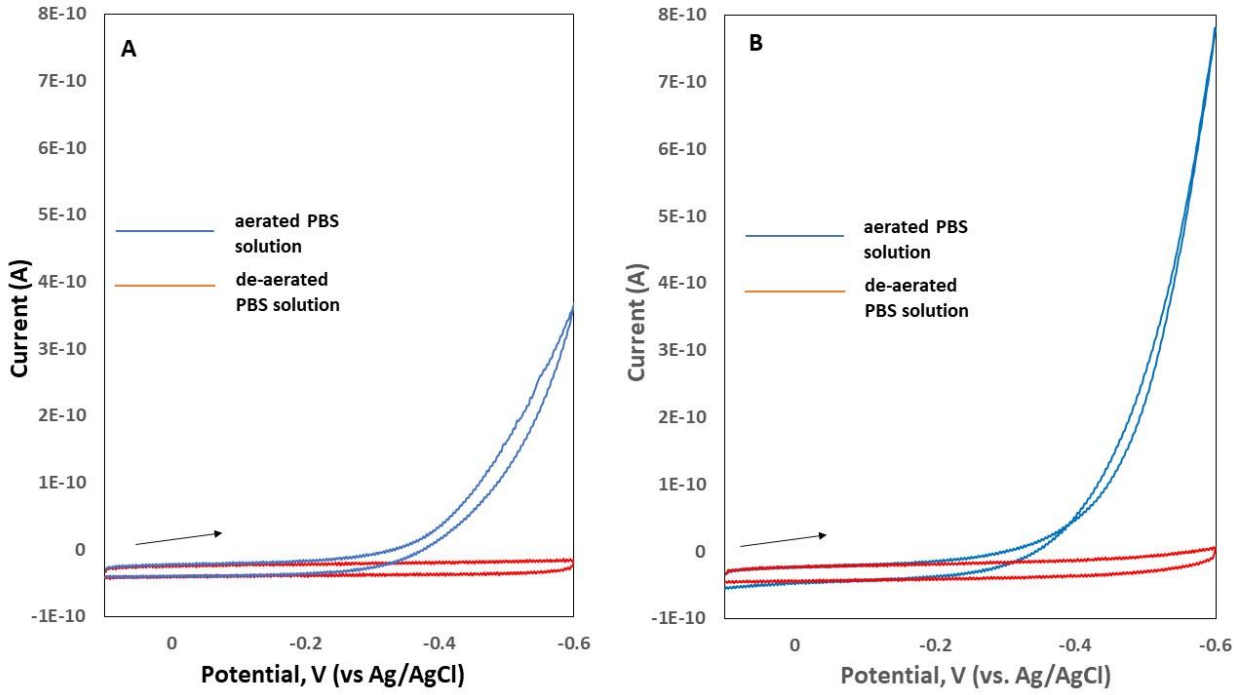

Figure 3. Representative cyclic voltammograms in aerated and de-aerated PBS pH 7.4 solution vs Ag/AgCl. (a) CF-UME (6.7 µm) and (b) N-CF-UME (6.4 µm). The arrows show the direction of the forward scan.

Comparison Between Solution-Based and Solid Urea Nitriding Methods

Members of the Bishop research group previously showed that the soft nitriding method developed by Liu et al.[67] for carbon black and mesoporous carbons could be successfully applied to graphite[76] and carbon fiber.[77] The simple strategy involves the thermal decomposition of solid urea in the presence of carbon material. Interestingly, Amoah[75] found that a similar strategy could be applied to pyrolytic carbon UMEs prepared via chemical vapor deposition. However, since such carbon UMEs are prepared by deposition of carbon directly in pulled glass capillaries, which are very fragile, urea solutions were used instead of solid urea. To evaluate how electrodes modified using solution-based urea nitriding compared to solid urea nitriding, reduction of hydrogen peroxide using nitrogen-doped carbon fiber UMEs prepared from the solution-based urea and solid urea (soft nitriding) were compared (Figure 4). For the solution-based nitriding,

carbon fiber was mixed with urea solution and heated to dryness using the same carbon fiber-to-urea mass ratio (1:1.5) and heating protocol for typical soft nitriding.

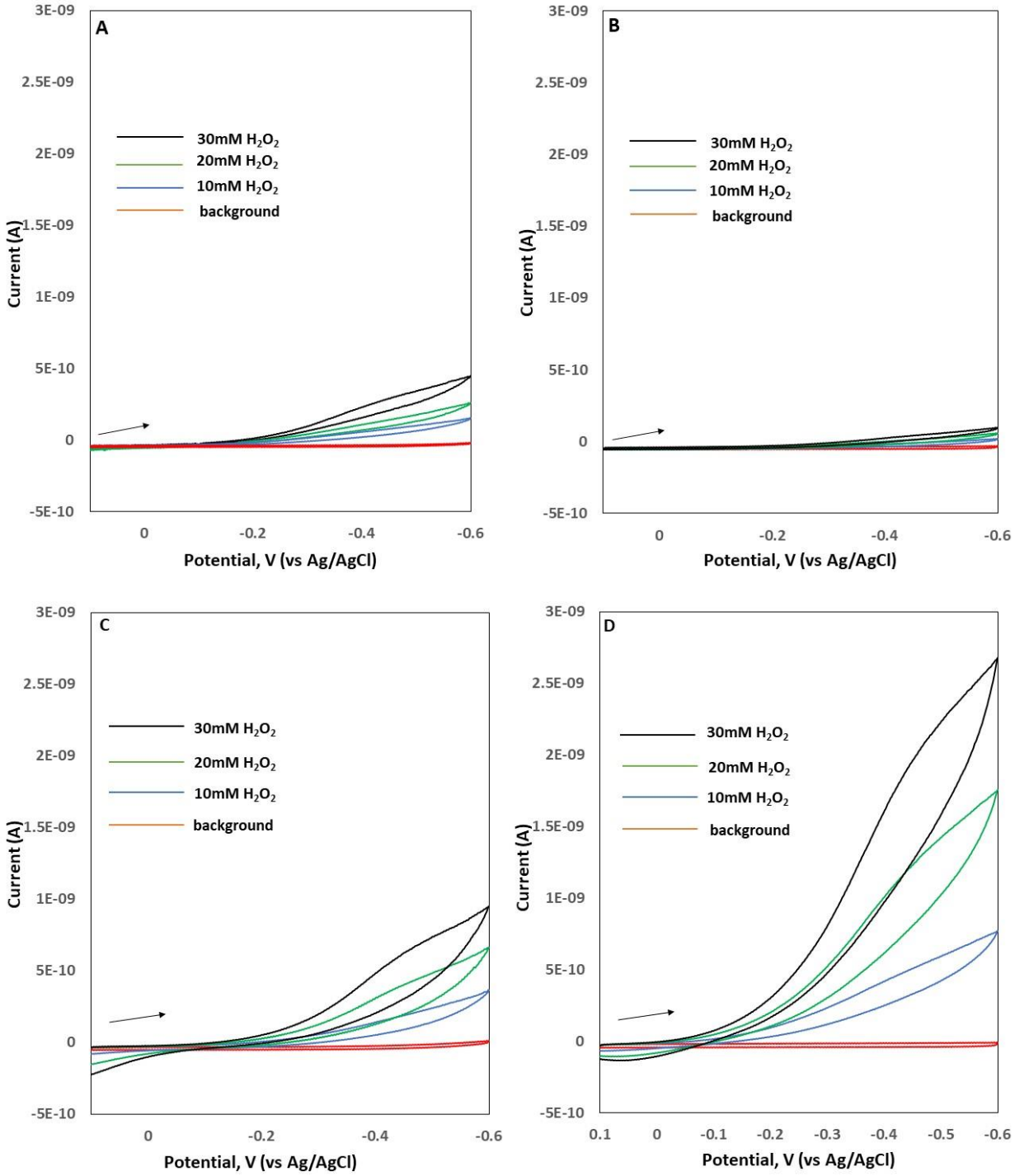

Figure 4. Representative cyclic voltammogram in PBS pH 7.4 solution vs Ag/AgCl. (a) CF-UME 6.7 µm) (b) 0.4 M urea solution N-CF-UME (5.7 µm) (c) 1.6 M urea solution N-CF-UME (6.0 µm) (d) solid urea N-CF-UME (6.0 µm). The arrows show the direction of the forward scan.

The responses of CF-UMEs showed a current enhancement of about 2.8 times compared to that of 0.4 M urea solution N-CF-UME. This shows that CF-UMEs performs better than a 0.4 M urea solution N-CF-UME with a shift to a more positive onset potential. Such a low concentration of urea solution is detrimental to the performance of N-CF-UMEs towards H_2O_2 reduction. While the response of N-CF-UME fabricated from the 1.6 M urea solution produced a significant response compared to both the 0.4 M urea solution N-CF-UMEs and CF-UMEs, N-CF-UMEs prepared using solid urea (typical soft nitriding) showed the best electrocatalytic behavior towards reduction of H_2O_2. For electrodes of similar sizes, the current enhancement at the solid urea N-CF-UMEs is about 3.2 times compared to that of the solution-based N-CF-UMEs (1.6 M urea) at -0.4V.

The low electrocatalytic response of the solution-based N-CF-UMEs towards H_2O_2 reduction seems to indicate that the solution-based protocol is not as effective at introducing nitrogen groups on the surface of the carbon fiber. For the thermal decomposition of solid urea, a previous member of this group[77] demonstrated this method (soft nitriding) on carbon fiber. XPS results showed the presence of pyridinic nitrogen (54.48%), amine/amide nitrogen (40.59%), ammonium nitrogen (2.60%), and nitride (2.32%) on the carbon fiber. In a related thermal decomposition of solid urea on graphitic carbon by another member of this group[76], XPS results showed that besides isocyanic acid and ammonia that is produced, other product like 1,3,5-triazines are also produced through polymerization and condensation reactions of urea. In comparison to the thermal decomposition of urea in water, isocyanic acid and ammonia so far have been reported to be the main products formed and this is supported by equations (4) and (5).[82]

$$(NH_2)_2CO(aq) \rightarrow (NH_2)_2CO(s) + xH_2O(l) \qquad (4)$$

$$(NH_2)_2CO(s) \rightarrow NH_3(g) + HNCO(g) \qquad (5)$$

In another related thermal decomposition of aqueous urea, Zhuang et al.[83] reported an increase in yield of ammonia at the temperature ranging from 473 K to 923 K which remained at about 60% as the temperature increased from 923 K to 1073 K in the absence of a catalyst. By this, we believed there was an increase in the amount of ammonia present on our solution-based nitrided carbon fiber since we used a temperature of 523.15 K in the absence of a catalyst. The low catalytic activity of the solution-based N-CF-UMEs could be attributed to the absence of these other products in the solution-based nitriding that were otherwise produced in the thermal decomposition of solid urea. These products are believed to enhance the nitrogen doping process of carbon materials[84] and therefore resulting in the improved electrocatalytic activity of solid urea N-CF-UMEs towards H_2O_2 reduction compared to the solution-based urea N-CF-UMEs.

Comparing both nitriding protocols, solid urea nitriding produced better electrocatalytic results. Therefore N-CF-UMEs prepared using solid urea were used for all further studies.

CF-UMEs and N-CF-UMEs Response towards Hydrogen Peroxide Reduction

The electrochemical responses of both CF-UMEs and N-CF-UMEs towards varying concentrations of H_2O_2 (5 mM, 10 mM, 15 mM, and 20 mM) in de-aerated PBS solution were evaluated (Figure 5). At each time of injection, N_2 gas was bubbled into the solution for 20 minutes and the solution was held under N_2 atmosphere before electrochemical measurements were made. CVs of similarly sized CF-UME (5.0 µm) and N-CF-UME (5.1 µm) in the presence of H_2O_2 confirm the nitrogen doping process enhances electrocatalytic activity for reduction of H_2O_2. Compared to CF-UME, reduction of hydrogen peroxide at N-CF-UME resulted in a current that is 5 to 7 times larger at -0.4 V vs Ag/AgCl. The reduction of H_2O_2 is commonly

observed at -0.4 V.[76] Also, a shift to a more positive onset potential for the reaction can be observed for N-CF-UME (5.0 µm) compared to CF-UME (5.1 µm).

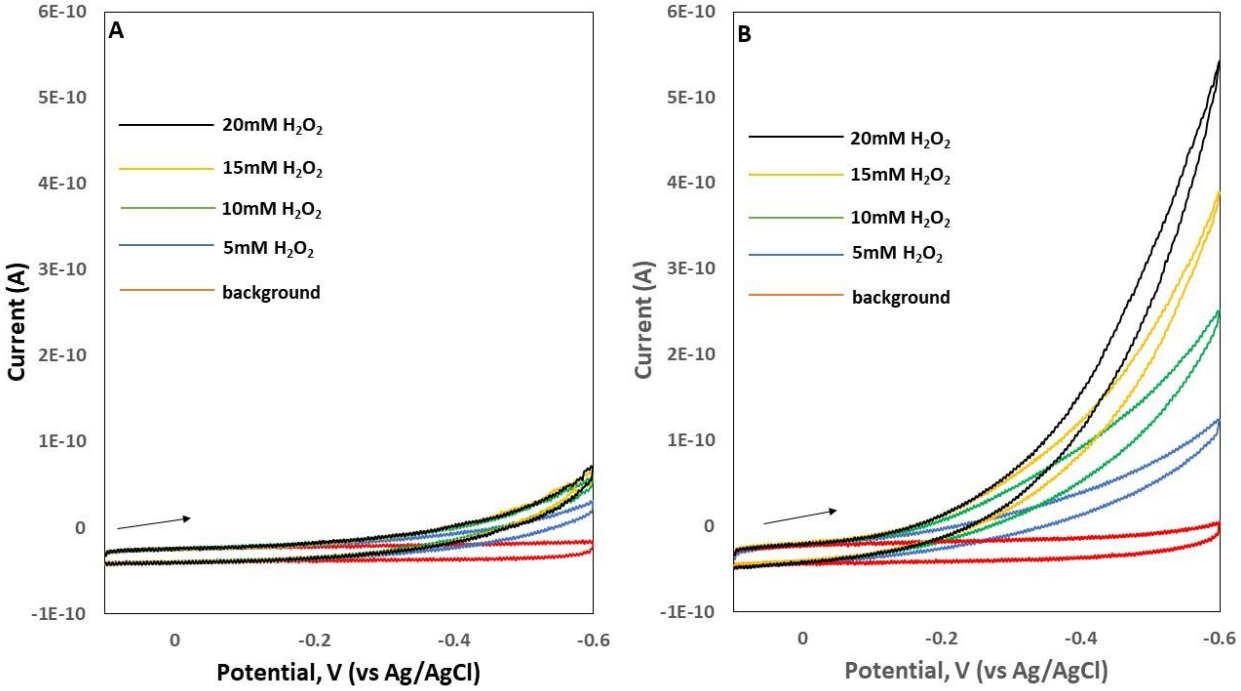

Figure 5. Representative cyclic voltammograms of varying concentrations of H_2O_2 in PBS pH 7.4 vs Ag/AgCl.(a) CF-UMEs (5.0 µm) (b) N-CF-UMEs (5.1 µm). The arrows show the direction of the forward scan.

Overall, the electrochemical performances of N-CF-UMEs showed improved electrocatalytic responses towards H_2O_2 reduction compared to CF-UMEs within the size range 3 µm to 7 µm (Figure 6). While a constant H_2O_2 reduction current density for N-CF-UMEs regardless of size would suggest N-doping was uniform over the electrode surface, a fairly linear relationship (R^2 = 0.9355) between electrode size and reduction current density was obtained instead. Based on the CV data, larger N-CF-UMEs gave an enhanced voltammetric response towards H_2O_2 reduction currents. This may suggest that larger electrodes exhibited a higher density of electrocatalytic active nitrogen groups, or such groups were not completely exposed during the polishing process for smaller electrodes.

For amperometric detection both N-CF-UMEs and CF-UMEs of similar sizes ≥5 µm that produced a high electrochemical response for cyclic voltammetry were used.

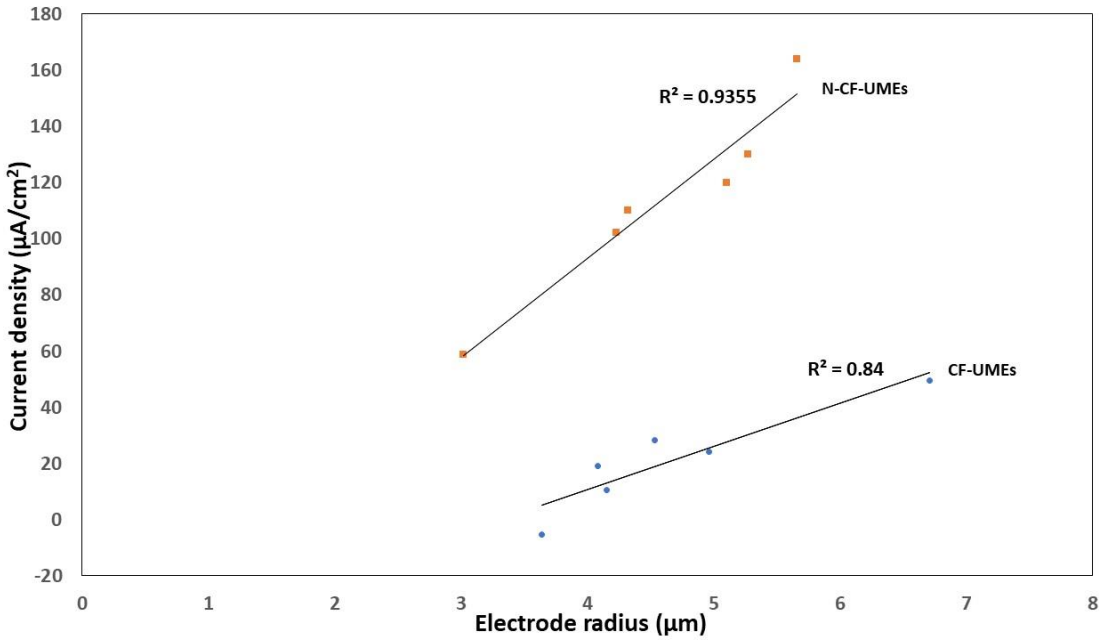

Figure 6. Effect of UME size on CV current density associated with reduction of H_2O_2 at -0.4 V.

Amperometric Detection of H_2O_2 Using CF-UMEs and N-CF-UMEs

Amperometric responses of both CF-UMEs and N-CF-UMEs towards H_2O_2 were evaluated at an applied potential of -0.4 V with varying concentrations of H_2O_2 in PBS pH 7.4 solution (Figure 7). Before each injection of hydrogen peroxide, an equal volume of buffer was injected to evaluate background current stability.

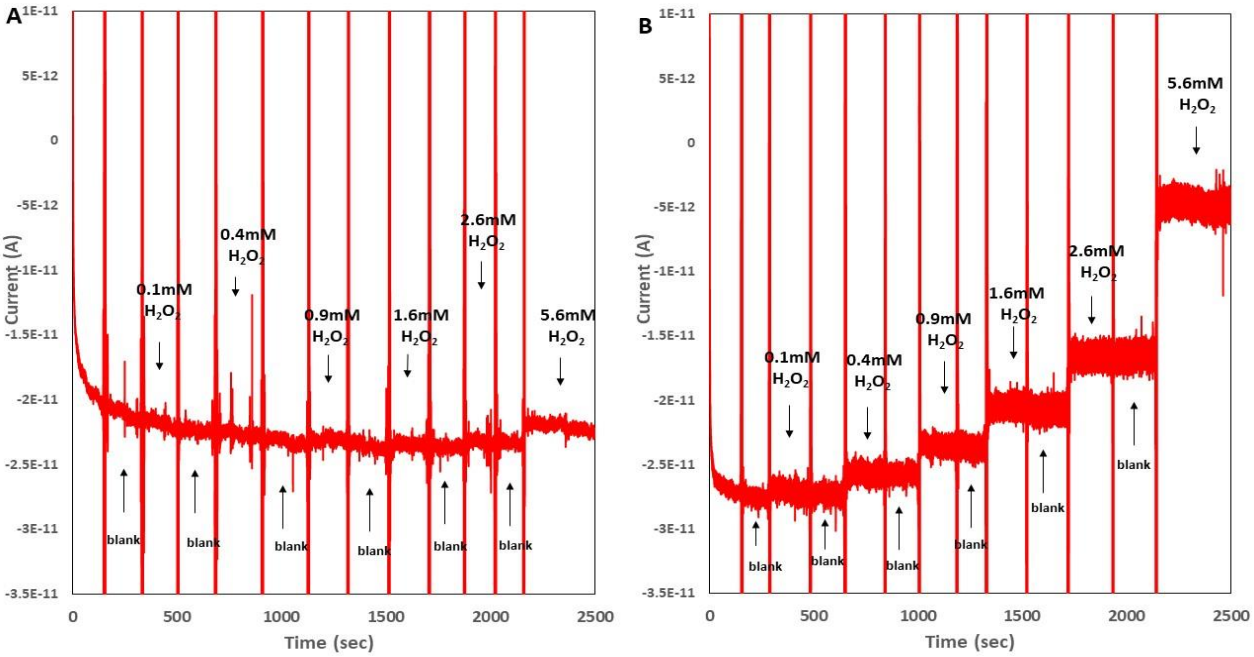

Figure 7. Amperometry detection of H_2O_2 in PBS pH 7.4 at -0.4 V vs. Ag/AgCl. (a) CF-UME (5.0 µm) (b) N-CF-UME (5.1 µm)

Vertical lines observed at the time of each injection are due to noises that are introduced upon the opening and closing of the Faraday cage at each point of injection. Blank injections show no significant change in current compared to the background, but current was found to increase upon injection of sufficient H_2O_2, which can be attributed to the reduction of H_2O_2 occurring at the electrode surface. CF-UMEs showed no significant change in current response upon the injection of H_2O_2 until the concentration exceeded 5 mM, whereas N-CF-UMEs showed an increase in current response when as little as 100 µM was H_2O_2 was present in the solution.

The calibration curve for amperometric detection of hydrogen peroxide using N-CF-UME (Figure 8) shows an excellent linear relationship between response and concentrations in the range of 0.1 mM to 5.6 mM H_2O_2 for N-CF-UMEs with an R^2 value of 0.9981. The sensitivity of the N-CF-UME based on the slope of the calibration curve was found to be 5.5 µA

mM^{-1} cm^{-2}. This is about 50 times lower compared to the lowest sensitivity reported (Table 1) although many others did not report their sensitivities. While the sensitivity of N-CF-UMEs is low compared to the other CF-UMEs (Table 1) which are in the range 273 to 7711 µA mM^{-1} cm^{-2}, the high sensitivities are due to surface modifications with metals, metal nanoparticles, enzymes, and biomolecules. The detection limit calculated based on three times the standard deviation of the background current as the minimum detectable signal was 137 µM. This is also about 1,000 to 2,000 times higher compared to the lowest reported detection limit (Table 1). The range of detection limits reported is 0.07 to 44 µM (Table 1).

Overall while N-CF-UMEs did show enhanced voltammetric response towards H_2O_2 reduction compared to CF-UMEs, the amperometric response towards H_2O_2 reduction was not as promising as some other methods. With the high detection limit, it might be able to have applications where concentrations of H_2O_2 are expected to be higher than 100 µM.

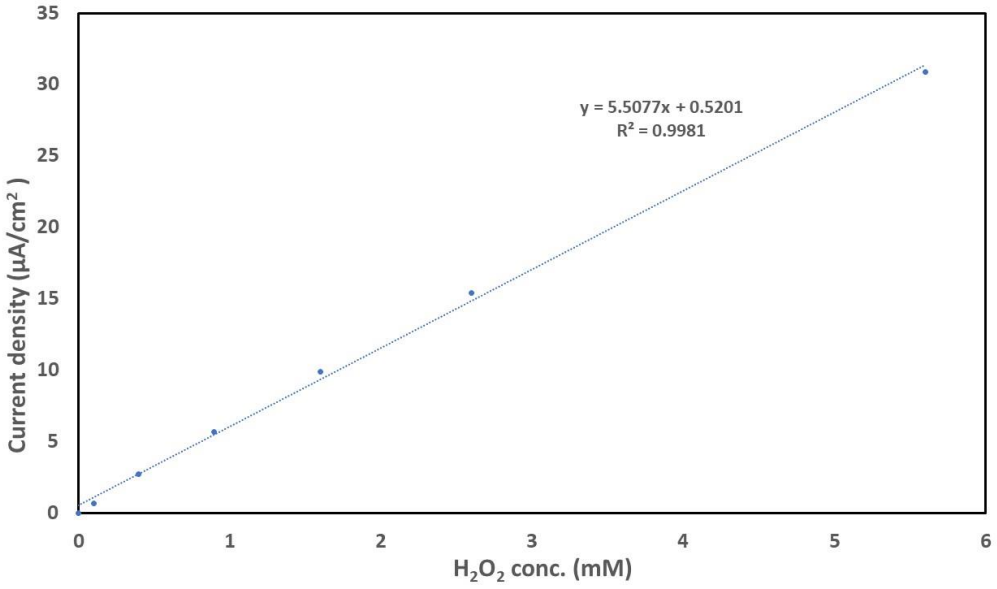

Figure 8. Representative calibration curve for amperometric detection of H_2O_2 in PBS pH 7.4 at -0.4V vs. Ag/AgCl. for N-CF-UME (5.1 µm)

CHAPTER 4. CONCLUSION AND FUTURE WORK

Conclusion

In this study, nitrogen doping of carbon fiber was evaluated as a strategy of sensing hydrogen peroxide electrochemically. CF-UMEs and N-CF-UMEs were prepared using a laser-based pipet puller. Electrode sizes in the range of 3 µm to 7 µm were fabricated and characterized by cyclic voltammetry. Cyclic voltammograms of the electrocatalytic activity of both electrodes in PBS solution towards dissolved oxygen in air showed that N-CF-UMEs produced an enhanced current of about 2.5 times compared to CF-UMEs. Reduction reactions of varying concentrations of H_2O_2 in PBS pH 7.4 were carried out using cyclic voltammetry for both CF-UMEs and N-CF-UMEs. The current enhancement at N-CF-UMEs was about 5 to 7 times greater compared to CF-UMEs. Amperometric responses of both CF-UMEs and N-CF-UMEs towards hydrogen peroxide were also evaluated. While N-CF-UMEs showed a current response when as little as 0.1 mM H_2O_2 was injected, CF-UMEs showed a current response when H_2O_2 concentration above 5 mM was injected. The sensitivity and detection limit of N-CF-UMEs were 5.5 µA mM^{-1} cm^{-2} and 137 µM respectively.

Overall N-CF-UMEs showed an enhanced electrocatalytic activity towards hydrogen peroxide for both voltammetric and amperometric measurements compared to CF-UMEs. This can be attributed to the presence of nitrogen groups on N-CF-UMEs which is believed to facilitate the breakage of the O-O bonds.[70,71] Although both CF-UMEs and N-CF-UMEs having radii <5 µm produced voltammetric responses, such electrodes especially CF-UMEs does not produce any observable amperometric responses.

Future Work

Though N-CF-UMEs showed an enhanced electrocatalytic response towards hydrogen peroxide compared to CF-UMEs, these electrodes are not sensitive enough compared to the sensitivities produce by carbon fiber UMEs modified using other modifications strategies (Table 1). While nitrogen doping does not seem to be a viable strategy for modifying carbon fiber UMEs to be used as sensors for H_2O_2, enhancement of these sensing properties might be possible by incorporating other kinds of modification strategies such as metal nano-particles. Nitrogen doping of carbon materials has been shown to enable the *in situ* growth of ligand-free ultrasmall (less than 2 nm) of electroactive metal nanoparticles onto carbon[67], metal nanoparticle modified N-CF-UMEs can therefore be fabricated and this may significantly enhance the sensitivity as well as the detection limit of N-CF-UMEs.

REFERENCES

1. Zoski, C. G. Ultramicroelectrodes: Design, Fabrication, and Characterization. Electroanalysis 2002, 14 (15–16), 1041–1051. https://doi.org/10.1002/1521-4109(200208)14:15/16<1041: AID-ELAN1041>3.0.CO;2-8.

2. Pons, S.; Fleischmann, M. The Behavior of Microelectrodes. ACS 1987, 59 (24), 1391A-1399A. https://doi.org/10.1021/ac00151a001.

3. Bard, A. J.; R.Faulkner, L. ELECTROCHEMICAL METHODS : Fundamentals and Applications, 2nd ed.; John Wiley & Sons: New York: Wiley, 2001.

4. J.Forster, R.; E.Keyes, T. Handbook of Electrochemistry; Zoski, C. G., Ed.; Elsevier B.V., 2007. https://doi.org/10.1016/B978-044451958-0.50007-0.

5. Forster, R. J. Microelectrodes: New Dimensions in Electrochemistry. Chem. Soc. Rev. 1994, 23 (4), 289–297. https://doi.org/10.1039/CS9942300289.

6. Bond, A. M.; Fleischmann, M.; Robinson, J. Electrochemistry in Organic Solvents without Supporting Electrolyte Using Platinum Microelectrodes. J. Electroanal. Chem. 1984, 168 (1–2), 299–312. https://doi.org/10.1016/0368-1874(84)87106-3.

7. Wightman, R. M. Microvoltammetric Electrodes. Anal. Chem. 1981, 53 (9), 1125A-1134A. https://doi.org/10.1021/ac00232a791.

8. Chen, Y.; Li, Q.; Jiang, H.; Wang, X. Pt Modified Carbon Fiber Microelectrode for Electrochemically Catalytic Reduction of Hydrogen Peroxide and Its Application in Living Cell H2O2 Detection. J. Electroanal. Chem. 2016, 781, 233–237. https://doi.org/10.1016/j.jelechem.2016.06.020.

9. Eklund, J. C.; Bond, A. M.; Alden, J. A.; Compton, R. G. Perspectives in Modern Voltammetry: Basic Concepts and Mechanistic Analysis. Adv. Phys. Org. Chem. 1999, 32 (C), 1–120. https://doi.org/10.1016/S0065-3160(08)60006-4

10. Heinze, J. Ultramicroelectrodes in Electrochemistry. Angew. Chemie - Int. Ed. 1993, 32 (9), 1268–1288. https://doi.org/10.1002/anie.199312681.

11. Bard, A. J.; Fan, F. R. F.; Kwak, J.; Lev, O. Scanning Electrochemical Microscopy. Introduction and Principles. Anal. Chem. 1989, 61 (2), 132–138. https://doi.org/10.1021/ac00177a011.

12. Satpati, A. K.; Bard, A. J. Preparation and Characterization of Carbon Powder Paste Ultramicroelectrodes as Tips for Scanning Electrochemical Microscopy Applications. Anal. Chem. 2012, 84 (21), 9498–9504. https://doi.org/10.1021/ac302349m.

13. Holt, K. B.; Hu, J.; Foord, J. S. Fabrication of Boron-Doped Diamond Ultramicroelectrodes for Use in Scanning Electrochemical Microscopy Experiments. Anal. Chem. 2007, 79 (6), 2556–2561. https://doi.org/10.1021/ac061995s.

14. Anderson, T. J.; Zhang, B. Single-Nanoparticle Electrochemistry through Immobilization and Collision. Acc. Chem. Res. 2016, 49 (11), 2625–2631. https://doi.org/10.1021/acs.accounts.6b00334.

15. Xiao, Y.; Fan, F. R. F.; Zhou, J.; Bard, A. J. Current Transients in Single Nanoparticle Collision Events. J. Am. Chem. Soc. 2008, 130 (49), 16669–16677. https://doi.org/10.1021/ja8051393.

16. Kwon, S. J.; Fan, F. R. F.; Bard, A. J. Observing Iridium Oxide (IrOx) Single Nanoparticle Collisions at Ultramicroelectrodes. J. Am. Chem. Soc. 2010, 132 (38), 13165–13167. https://doi.org/10.1021/ja106054c.

17. Zhou, H.; Park, J. H.; Fan, F. R. F.; Bard, A. J. Observation of Single Metal Nanoparticle Collisions by Open Circuit (Mixed) Potential Changes at an Ultramicroelectrode. J. Am. Chem. Soc. 2012, 134 (32), 13212–13215. https://doi.org/10.1021/ja305573g.

18. Katemann, B. B.; Schuhmann, W. Fabrication and Characterization of Needle-Type Pt-disk Nanoelectrodes Electroanalysis 2002, 14 (1), 22–28. https://doi.org/10.1002/1521-4109(200201)14:1%3C22::aid-elan22%3E3.0.co;2-f.

19. Danis, L.; Snowden, M. E.; Tefashe, U. M.; Heinemann, C. N.; Mauzeroll, J. Development of Nano-Disc Electrodes for Application as Shear Force Sensitive Electrochemical Probes. Electrochim. Acta 2014, 136, 121–129. https://doi.org/10.1016/j.electacta.2014.05.047.

20. Harvey, S. L. R.; Coxon, P.; Bates, D.; Parker, K. H.; O'Hare, D. Metallic Ring-Disc Microelectrode Fabrication Using Inverted Hollow Cylindrical Sputter Coater. Sensors Actuators, B Chem. 2008, 129 (2), 659–665. https://doi.org/10.1016/j.snb.2007.09.019.

21. Liljeroth, P.; Johans, C.; Slevin, C. J.; Quinn, B. M.; Kontturi, K. Micro Ring-Disk Electrode Probes for Scanning Electrochemical Microscopy. Electrochem. commun. 2002, 4 (1), 67–71. https://doi.org/10.1016/s1388-2481(01)00276-4.

22. Mauzeroll, J.; Hueske, E. A.; Bard, A. J. Scanning Electrochemical Microscopy. 48. Hg/Pt Hemispherical Ultramicroelectrodes: Fabrication and Characterization. Anal. Chem. 2003, 75 (15), 3880–3889. https://doi.org/10.1021/ac034088l.

23. Velmurugan, J.; Noël, J. M.; Mirkin, M. V. Nucleation and Growth of Mercury on Pt Nanoelectrodes at Different Overpotentials. Chem. Sci. 2014, 5 (1), 189–194. https://doi.org/10.1039/c3sc52488d.

24. V.Mirkin, M.; F.Fan, F.-R.; J.Bard, A. Scanning Electrochemical Microscopy Part 13. Evaluation of the Tip Shapes of Nanometer Size Microelectrodes. J. Electroanal. Chem. 1992, 328 (1–2), 47–62. https://doi.org/10.1016/0022-0728(92)80169-5.

25. Takahashi, Y.; Shevchuk, A. I.; Novak, P.; Murakami, Y.; Shiku, H.; Korchev, Y. E.; Matsue, T. Simultaneous Noncontact Topography and Electrochemical Imaging by SECM/SICM Featuring Ion Current Feedback Regulation. J. Am. Chem. Soc. 2010, 132 (29), 10118–10126. https://doi.org/10.1021/ja1029478.

26. Lee, Y.; Bard, A. J. Fabrication and Characterization of Probes for Combined Scanning Electrochemical/Optical Microscopy Experiments. Anal. Chem. 2002, 74 (15), 3626 – 3633. https://doi.org/10.1021/ac015705d.

27. Danis, L.; Polcari, D.; Kwan, A.; Gateman, S. M.; Mauzeroll, J. Fabrication of Carbon, Gold, Platinum, Silver, and Mercury Ultramicroelectrodes with Controlled Geometry. Anal. Chem. 2015, 87 (5), 2565–2569. https://doi.org/10.1021/ac503767n.

28. Noël, J. M.; Velmurugan, J.; Gökmeşe, E.; Mirkin, M. V. Fabrication, Characterization, and Chemical Etching of Ag Nanoelectrodes. J. Solid State Electrochem. 2013, 17 (2), 385–389. https://doi.org/10.1007/s10008-012-1849-6.

29. Zoski, C. G. Handbook of Electrochemistry, 1st ed.; Elsevier: Oxford, 2007.

30. Dayton, M. A.; Brown, J. C.; Stutts, K. J.; Wightman, R. M. Faradaic Electrochemistry at Microvoltammetric Electrodes. Anal. Chem. 1980, 52 (6), 946–950. https://doi.org/10.1021/ac50056a040.

31. Robinson, R. S.; McCreery, R. L. Absorption Spectroelectrochemistry with Microelectrodes. Anal. Chem. 1981, 53 (7), 997–1001. https://doi.org/10.1021/ac00230a017.

32. Gajovic-Eichelmann, N.; Ehrentreich-Förster, E.; Bier, F. F. Directed Immobilization of Nucleic Acids at Ultramicroelectrodes Using a Novel Electro-Deposited Polymer. Biosens. Bioelectron. 2003, 19 (5), 417–422. https://doi.org/10.1016/s0956-5663(03)00224-0.

33. Carrera, P.; Espinoza-Montero, P. J.; Fernández, L.; Romero, H.; Alvarado, J. Electrochemical Determination of Arsenic in Natural Waters Using Carbon Fiber Ultra-Microelectrodes Modified with Gold Nanoparticles. Talanta 2017, 166 (November 2016), 198–206. https://doi.org/10.1016/j.talanta.2017.01.056.

34. Orozco, J.; Jiménez-Jorquera, C.; Fernández-Sánchez, C. Gold Nanoparticle-Modified Ultramicroelectrode Arrays for Biosensing: A Comparative Assessment. Bioelectrochemistry 2009, 75 (2), 176–181. https://doi.org/10.1016/j.bioelechem.2009.03.013.

35. Li, J.; Yu, J. Fabrication of Prussian Blue Modified Ultramicroelectrode for GOD Imaging Using Scanning Electrochemical Microscopy. Bioelectrochemistry 2008, 72 (1), 102–106. https://doi.org/10.1016/j.bioelechem.2007.11.013.

36. Qing, W.; Liu, X.; Lu, H.; Liang, J.; Liu, K. Ensemble of Carbon Fiber Ultra-Microelectrodes Modified with Nanotubes, and Its Application to the Determination of Dopamine. Microchim. Acta 2008, 160 (1–2), 227–231. https://doi.org/10.1007/s00604-007-0826-8.

37. Pollack, B.; Holmberg, S.; George, D.; Tran, I.; Madou, M.; Ghazinejad, M. Nitrogen-Rich Polyacrylonitrile-Based Graphitic Carbons for Hydrogen Peroxide Sensing. Sensors (Switzerland) 2017, 17 (10), 1–12. https://doi.org/10.3390/s17102407.

38. Chen, W.; Cai, S.; Ren, Q. Q.; Wen, W.; Zhao, Y. Di. Recent Advances in Electrochemical Sensing for Hydrogen Peroxide: A Review. Analyst 2012, 137 (1), 49–58. https://doi.org/10.1039/c1an15738h.

39. Lee, C. R.; Patel, J. C.; O'Neill, B.; Rice, M. E. Inhibitory and Excitatory Neuromodulation by Hydrogen Peroxide: Translating Energetics to Information. J. Physiol. 2015, 593 (16), 3431–3446. https://doi.org/10.1113/jphysiol.2014.273839.

40. Mao, Y.; Bao, Y.; Wang, W.; Li, Z.; Li, F.; Niu, L. Layer-by-Layer Assembled Multilayer of Graphene/Prussian Blue toward Simultaneous Electrochemical and SPR Detection of H2O2. Talanta 2011, 85 (4), 2106–2112. https://doi.org/10.1016/j.talanta.2011.07.056.

41. Higashi, N.; Yokota, H.; Hiraki, S.; Ozaki, Y. Direct Determination of Peracetic Acid, Hydrogen Peroxide, and Acetic Acid in Disinfectant Solutions by Far-Ultraviolet Absorption Spectroscopy. Anal. Chem. 2005, 77 (7), 2272–2277. https://doi.org/10.1021/ac0487045.

42. Chang, M. C. Y.; Pralle, A.; Isacoff, E. Y.; Chang, C. J. A Selective, Cell-Permeable Optical Probe for Hydrogen Peroxide in Living Cells. J. Am. Chem. Soc. 2004, 126 (47), 15392 – 15393. https://doi.org/10.1021/ja0441716.

43. Chen, S.; Yuan, R.; Chai, Y.; Zhang, L.; Wang, N.; Li, X. Amperometric Third-Generation Hydrogen Peroxide Biosensor Based on the Immobilization of Hemoglobin on Multiwall Carbon Nanotubes and Gold Colloidal Nanoparticles. Biosens. Bioelectron. 2007, 22 (7), 1268–1274. https://doi.org/10.1016/j.bios.2006.05.022.

44. Liu, C. Y.; Hu, J. M. Hydrogen Peroxide Biosensor Based on the Direct Electrochemistry of Myoglobin Immobilized on Silver Nanoparticles Doped Carbon Nanotubes Film. Biosens. Bioelectron. 2009, 24 (7), 2149–2154. https://doi.org/10.1016/j.bios.2008.11.007.

45. Goran, J. M.; Phan, E. N. H.; Favela, C. A.; Stevenson, K. J. H2O2 Detection at Carbon Nanotubes and Nitrogen-Doped Carbon Nanotubes: Oxidation, Reduction, or Disproportionation? Anal. Chem. 2015, 87 (12), 5989–5996. https://doi.org/10.1021/acs.analchem.5b00059.

46. Lin, J.; Xin, Q.; Gao, X. Real-Time Detection of Hydrogen Peroxide Using Microelectrodes in an Ultrasonic Enhanced Heterogeneous Fenton Process Catalyzed by Ferrocene. Environ. Sci. Pollut. Res. 2015, 22 (14), 11170–11174. https://doi.org/10.1007/s11356-015-4774-2.

47. Skoog, D. A.; Holler, F. J.; Crouch, S. R. Principles of Instrumental Analysis, 7th ed.; Cengage Learning: Boston, MA, 2018.

48. Zheng, Y. L.; Mei, D.; Chen, Y. X.; Ye, S. The Redox Reaction of Hydrogen Peroxide at an Au (100) Electrode: Implications for Oxygen Reduction Kinetics. Electrochem. commun. 2014, 39, 19–21. https://doi.org/10.1016/j.elecom.2013.12.005.

49. Xu, S.; Zhang, X.; Wan, T.; Zhang, C. A Third-Generation Hydrogen Peroxide Biosensor Based on Horseradish Peroxidase Cross-Linked to Multi-Wall Carbon Nanotubes. *Microchim. Acta* **2011**, *172* (1), 199–205. https://doi.org/10.1007/s00604-010-0479-x.

50. Liu, Y.; Wang, D.; Xu, L.; Hou, H.; You, T. A Novel and Simple Route to Prepare a Pt Nanoparticle-Loaded Carbon Nanofiber Electrode for Hydrogen Peroxide Sensing. Biosens. Bioelectron. 2011, 26 (11), 4585–4590. https://doi.org/10.1016/j.bios.2011.05.034.

51. Li, C. M.; Hu, W. Electroanalysis in Micro- and Nano-Scales. J. Electroanal. Chem. 2013, 688, 20–31. https://doi.org/10.1016/j.jelechem.2012.07.010.

52. Chang, M. L.; Zang, J.; Zhan, D.; Chen, W.; Sun, C. Q.; Teo, A. L.; Chua, Y. T.; Lee, V. S.; Moochhala, S. M. Electrochemical Detection of Nitric Oxide on a SWCNT/RTIL Composite Gel Microelectrode. Electroanalysis 2006, 18 (7), 713–718. https://doi.org/10.1002/elan.200503457.

53. Dantas, L. M. F.; Castro, P. S.; Peña, R. C.; Bertotti, M. Amperometric Determination of Hydrogen Peroxide Using a Copper Microelectrode. Anal. Methods 2014, 6 (7), 2112–2116. https://doi.org/10.1039/c3ay41980k.

54. Evans, S. A. G.; Elliott, J. M.; Andrews, L. M.; Bartlett, P. N.; Doyle, P. J.; Denuault, G. Detection of Hydrogen Peroxide at Mesoporous Platinum Microelectrodes. Anal. Chem. 2002, 74 (6), 1322–1326. https://doi.org/10.1021/ac011052p.

55. Liu, Y.; Sun, G.; Jiang, C.; Zheng, X. T.; Zheng, L.; Li, C. M. Highly Sensitive Detection of Hydrogen Peroxide at a Carbon Nanotube Fiber Microelectrode Coated with Palladium Nanoparticles. Microchim. Acta 2014, 181 (1–2), 63–70. https://doi.org/10.1007/s00604-013-1066-8.

56. Seven, F.; Gölcez, T.; ŞEN, M. Nanoporous Carbon-Fiber Microelectrodes for Sensitive Detection of H2O2 and Dopamine. J. Electroanal. Chem. 2020, 864, 114104. https://doi.org/10.1016/j.jelechem.2020.114104.

57. Sanford, A. L.; Morton, S. W.; Whitehouse, K. L.; Oara, H. M.; Lugo-Morales, L. Z.; Roberts, J. G.; Sombers, L. A. Voltammetric Detection of Hydrogen Peroxide at Carbon Fiber Microelectrodes. Anal. Chem. 2010, 82 (12), 5205–5210. https://doi.org/10.1021/ac100536s.

58. Seven, F.; Gölcez, T.; ŞEN, M. Nanoporous Carbon-Fiber Microelectrodes for Sensitive Detection of H2O2 and Dopamine. J. Electroanal. Chem. 2020, 864, 114104. https://doi.org/10.1016/j.jelechem.2020.114104.

59. Ledo, A.; Fernandes, E.; Brett, C. M. A.; Barbosa, R. M. Enhanced Selectivity and Stability of Ruthenium Purple-Modified Carbon Fiber Microelectrodes for Detection of Hydrogen Peroxide in Brain Tissue. Sensors Actuators, B Chem. 2020, 311 (February), 127899. https://doi.org/10.1016/j.snb.2020.127899.

60. Chen, S.; Yuan, R.; Chai, Y.; Hu, F. Electrochemical Sensing of Hydrogen Peroxide Using Metal Nanoparticles: A Review. Microchim. Acta 2013, 180 (1–2), 15–32. https://doi.org/10.1007/s00604-012-0904-4.

61. Wang, B.; Wen, X.; Chiou, P. Y.; Maidment, N. T. Pt Nanoparticle-Modified Carbon Fiber Microelectrode for Selective Electrochemical Sensing of Hydrogen Peroxide. Electroanalysis 2019, 31 (9), 1641–1645. https://doi.org/10.1002/elan.201900362.

62. Sun, W.; Cai, X.; Wang, Z.; Zhao, H.; Lan, M. A Novel Modification Method via In-Situ Reduction of AuAg Bimetallic Nanoparticles by Polydopamine on Carbon Fiber Microelectrode for H2O2 Detection. Microchem. J. 2020, 154, 104595. https://doi.org/10.1016/j.microc.2020.104595.

63. Kulagina, N. V.; Michael, A. C. Monitoring Hydrogen Peroxide in the Extracellular Space of the Brain with Amperometric Microsensors. Anal. Chem. 2003, 75 (18), 4875–4881. https://doi.org/10.1021/ac034573g.

64. Zhang, H.; Ruan, J.; Liu, W.; Jiang, X.; Du, T.; Jiang, H.; Alberto, P.; Gottschalk, K. E.; Wang, X. Monitoring Dynamic Release of Intracellular Hydrogen Peroxide through a Microelectrode Based Enzymatic Biosensor. Anal. Bioanal. Chem. 2018, 410 (18), 4509–4517. https://doi.org/10.1007/s00216-018-1108-5.

65. Shao, Y.; Zhang, S.; Engelhard, M. H.; Li, G.; Shao, G.; Wang, Y.; Liu, J.; Aksay, I. A.; Lin, Y. Nitrogen-Doped Graphene and Its Electrochemical Applications. J. Mater. Chem. 2010, 20 (35), 7491–7496. https://doi.org/10.1039/c0jm00782j.

66. Shi, L.; Niu, X.; Liu, T.; Zhao, H.; Lan, M. Electrocatalytic Sensing of Hydrogen Peroxide Using a Screen-Printed Carbon Electrode Modified with Nitrogen-Doped Graphene Nanoribbons. Microchim. Acta 2015, 182 (15–16), 2485–2493. https://doi.org/10.1007/s00604-015-1605-6.

67. Liu, B.; Yao, H.; Song, W.; Jin, L.; Mosa, I. M.; Rusling, J. F.; Suib, S. L.; He, J. Ligand-Free Noble Metal Nanocluster Catalysts on Carbon Supports via "Soft" Nitriding. J. Am. Chem. Soc. 2016, 138 (14), 4718–4721. https://doi.org/10.1021/jacs.6b01702.

68. Maldonado, S.; Stevenson, K. J. Direct Preparation of Carbon Nanofiber Electrodes via Pyrolysis of Iron (II) Phthalocyanine: Electrocatalytic Aspects for Oxygen Reduction. J. Phys. Chem. B 2004, 108 (31), 11375–11383. https://doi.org/10.1021/jp0496553.

69. Gong, K.; Du, F.; Xia, Z.; Durstock, M.; Dai, L. Nitrogen-Doped Carbon Nanotube Arrays with High Electrocatalytic Activity for Oxygen Reduction. Science (80-.). 2009, 323 (5915), 760–764. https://doi.org/10.1126/science.1168049.

70. Lyu, Y. P.; Wu, Y. S.; Wang, T. P.; Lee, C. L.; Chung, M. Y.; Lo, C. T. Hydrothermal and Plasma Nitrided Electrospun Carbon Nanofibers for Amperometric Sensing of Hydrogen Peroxide. Microchim. Acta 2018, 185 (8), 3–9. https://doi.org/10.1007/s00604-018-2915-2.

71. Lv, Q.; Si, W.; He, J.; Sun, L.; Zhang, C.; Wang, N.; Yang, Z.; Li, X.; Wang, X.; Deng, W.; Long, Y.; Huang, C.; Li, Y. Selectively Nitrogen-Doped Carbon Materials as Superior Metal-Free Catalysts for Oxygen Reduction. Nat. Commun. 2018, 9 (1). https://doi.org/10.1038/s41467-018-05878-y.

72. Dai, L.; Xue, Y.; Qu, L.; Choi, H. J.; Baek, J. B. Metal-Free Catalysts for Oxygen Reduction Reaction. Chem. Rev. 2015, 115 (11), 4823–4892. https://doi.org/10.1021/cr5003563.

73. Wu, P.; Du, P.; Zhang, H.; Cai, C. Microscopic Effects of the Bonding Configuration of Nitrogen-Doped Graphene on Its Reactivity toward Hydrogen Peroxide Reduction Reaction. Phys. Chem. Chem. Phys. 2013, 15 (18), 6920–6928. https://doi.org/10.1039/c3cp50900a.

74. Wang, Y.; Shao, Y.; Matson, D. W.; Li, J.; Lin, Y. Nitrogen-Doped Graphene and Its Biosensing. ACS Nano 2010, 4 (4), 1790–1798. https://doi.org/10.1063/1.4870424.

75. Amoah, E. Digital Commons @ East Tennessee State University Modification of Chemical Vapor-Deposited Carbon Electrodes with Electrocatalytic Metal Nanoparticles through a Soft Nitriding Technique. 2019.

76. Ogbu, C. I.; Feng, X.; Dada, S. N.; Bishop, G. W. Screen-Printed Soft-Nitrided Carbon Electrodes for Detection of Hydrogen Peroxide. Sensors (Switzerland) 2019, 19 (17), 1 – 16. https://doi.org/10.3390/s19173741

77. Affadu-danful, G. Immobilization of Gold Nanoparticles on Nitrided Carbon Fiber Ultramicroelectrodes by Direct Reduction. 2018, 46.

78. Fan, Y.; Han, C.; Zhang, B. Recent Advances in the Development and Application of Nanoelectrodes. Analyst 2016, 141 (19), 5474–5487. https://doi.org/10.1039/c6an01285j.

79. Elgrishi, N.; Rountree, K. J.; McCarthy, B. D.; Rountree, E. S.; Eisenhart, T. T.; Dempsey, J. L. A Practical Beginner's Guide to Cyclic Voltammetry. J. Chem. Educ. 2018, 95 (2), 197–206. https://doi.org/10.1021/acs.jchemed.7b00361.

80. Ying, Y. L.; Ding, Z.; Zhan, D.; Long, Y. T. Advanced Electroanalytical Chemistry at Nanoelectrodes. *Chem. Sci.* **2017**, *8* (5), 3338–3348. https://doi.org/10.1039/c7sc00433h.

81. Yu, Y.; Gao, Y.; Hu, K.; Blanchard, P. Y.; Noël, J. M.; Nareshkumar, T.; Phani, K. L.; Friedman, G.; Gogotsi, Y.; Mirkin, M. V. Electrochemistry and Electrocatalysis at Single Gold Nanoparticles Attached to Carbon Nanoelectrodes. ChemElectroChem 2015, 2 (1), 58–63. https://doi.org/10.1002/celc.201402312.

82. Koebel, M.; Strutz, E. O. Thermal and Hydrolytic Decomposition of Urea for Automotive Selective Catalytic Reduction Systems: Thermochemical and Practical Aspects. Ind. Eng. Chem. Res. 2003, 42 (10), 2093–2100. https://doi.org/10.1021/ie020950o.

83. Wang, D.; Hui, S.; Liu, C.; Zhuang, H. Effect of Oxygen and Additives on Thermal Decomposition of Aqueous Urea Solution. Fuel 2016, 180, 34–40. https://doi.org/10.1016/j.fuel.2016.04.018.

84. Schaber, P. M.; Colson, J.; Higgins, S.; Thielen, D.; Anspach, B.; Brauer, J. Thermal Decomposition (Pyrolysis) of Urea in an Open Reaction Vessel. Thermochim. Acta 2004, 424 (1–2), 131–142. https://doi.org/10.1016/j.tca.2004.05.018

VITA

ERIC SEDOM WORNYO

Education:

B.S. Chemistry, University of Cape-Coast, Cape-Coast, Ghana, 2011

M.S. Chemistry, East Tennessee State University, Johnson City, TN, 2021

Professional Experience:

Intern, Korle-Bu Teaching Hospital – Central Laboratory, Accra, Ghana
June 2010 – July 2010

Standards Officer, Ghana Standards Authority; Accra, Ghana
October 2011 -July 2012

Customer Service Representative, Tele Tech, Ghana
June 2013 – February 2014

Quality Control Analyst, Letap Pharmaceuticals Limited, Ghana
March 2014 – August 2019

Graduate Teaching Assistant, East Tennessee State University, Johnson City, TN
2019 – 2021

Research Assistant, East Tennessee State University,
(Supervisor: Dr. Gregory W. Bishop)

Research Experience:

Undergraduate Research Student, University of Cape – Coast, Cape – Coast, Ghana
2010 – 2011
(Supervisor: Dr. John K. Bentum)
Determined the effect of storage conditions on some quality parameters of palm kernel oil

Quality Control Analyst, Letap Pharmaceuticals Limited, Ghana
2017
1. Quantification of Artemether and Lumefantrine in fixed-dose combination using RP-HPLC with UV detection
2. Qualitative detection of Related substances in Artemether and Lumefantrine raw materials using TLC.

Research Assistant, East Tennessee State University,
Johnson City, TN
2019 – 2021
(Supervisor: Dr. Gregory W. Bishop)
Nitrogen-Doped Carbon Fiber Ultramicroelectrodes as Electrochemical Sensors for Detection of Hydrogen Peroxide

Community Outreach:

Ghana Student Chemical Society Conference Organizer, University of Cape – Coast, Ghana
2010

Health Sensitization and Screening Exercise for the Elderly and Aged
Ghana
2015 – 2018

Booth Volunteer, Graduate and Professional Student Association (GPSA), East Tennessee State University
March 2020

Honors and Awards:

The Margaret Sells Endowment Scholarship Award, Outstanding Achievement in the Field of Chemistry in the College of Arts and Sciences, East Tennessee State University,
Johnson City, TN
May – 15 – 2021